# Differential regulation of mast cell degranulation versus cytokine secretion by the actin regulatory proteins Coronin1a and Coronin1b

Niko Föger,[1] André Jenckel,[1] Zane Orinska,[1] Kyeong-Hee Lee,[1] Andrew C. Chan,[3] and Silvia Bulfone-Paus[1,2]

[1]Department of Immunology and Cell Biology, Research Center Borstel, 23845 Borstel, Germany
[2]School of Translational Medicine, The University of Manchester, M13 9PT Manchester, England, UK
[3]Department of Immunology, Genentech, South San Francisco, CA 94080

**Mast cell (MC) activation via aggregation of the high affinity IgE receptor (FcεRI) causes degranulation and release of proinflammatory mediators in a process that involves the reorganization of the actin cytoskeleton. However, the regulatory pathways and the molecular links between cytoskeletal changes and MC function are incompletely understood. In this study, we provide genetic evidence for a critical role of the actin-regulatory proteins Coronin1a (Coro1a) and Coro1b on exocytic pathways in MCs: *Coro1a*$^{-/-}$ bone marrow–derived MCs exhibit increased FcεRI-mediated degranulation of secretory lysosomes but significantly reduced secretion of cytokines. Hyperdegranulation of *Coro1a*$^{-/-}$ MCs is further augmented by the additional loss of Coro1b. In vivo, *Coro1a*$^{-/-}$*Coro1b*$^{-/-}$ mice displayed enhanced passive cutaneous anaphylaxis. Functional reconstitution assays revealed that the inhibitory effect of Coro1a on MC degranulation strictly correlates with cortical localization of Coro1a, requires its filamentous actin–binding activity, and is regulated by phosphorylation of Ser2 of Coro1a. Thus, coronin proteins, and in turn the actin cytoskeleton, exhibit a functional dichotomy as differential regulators of degranulation versus cytokine secretion in MC biology.**

CORRESPONDENCE
Niko Föger:
nfoeger@fz-borstel.de

Abbreviations used: BMMC, BM-derived MC; DNP-HSA, DNP human serum albumin; F-actin, filamentous actin; MC, mast cell; mRNA, messenger RNA; PCA, passive cutaneous anaphylaxis; PFA, paraformaldehyde.

Mast cells (MCs) are recognized to secrete a multitude of mediators, including cytokines and proteases, which enables them to play an important role in the initiation and maintenance of appropriate, selective, and effective immune responses as well as in allergic diseases (Blank and Rivera, 2004; Kinet, 2007; Brown et al., 2008; Kalesnikoff and Galli, 2008). Activation of MCs via FcεRI triggering causes the immediate degranulation and release of preformed mediators from secretory granules, as well as de novo synthesis of cytokines, which are secreted after vesicular trafficking via the ER and Golgi complex. Recent work acknowledges an important role of the actin cytoskeleton in MC exocytosis (Frigeri and Apgar, 1999; Nishida et al., 2005; Sasaki et al., 2005). However, controversial findings have raised questions regarding the specific function and regulation of the actin cytoskeleton in secretory processes (Eitzen, 2003; Malacombe et al., 2006).

Coronins constitute a family of evolutionary highly conserved WD repeat–containing proteins that have been implicated in the regulation of actin cytoskeletal dynamics (Uetrecht and Bear, 2006; Clemen et al., 2008). Diverse functions of coronin proteins on actin filaments have been reported, including actin binding/bundling, actin disassembly, and inhibition of the Arp2/3 complex (Humphries et al., 2002; Cai et al., 2007a,b; Galkin et al., 2008; Kueh et al., 2008; Gandhi et al., 2009). In mammalians, seven coronin family members have been described. A high degree of sequence similarities among coronin family proteins suggests

A. Jenckel and Z. Orinska contributed equally to this paper.
A.C. Chan and S. Bulfone-Paus contributed equally to this paper.



The Rockefeller University Press $30.00
J. Exp. Med. Vol. 208 No. 9 1777-1787
www.jem.org/cgi/doi/10.1084/jem.20101757

conserved features and functions. However, individual family members may have developed additional selective and specific functions. Based on their phylogenetic relationship, mammalian coronins have been divided into three different types: type I (Coro1a, Coro1b, Coro1c, and Coro6), type II (Coro2a and Coro2b), and type III (Coro7). In humans and mice, mutation or deletion of Coro1a, which is preferentially expressed in hematopoietic cells, results in a severe combined immunodeficiency that has mainly been attributed to defective actin regulation in T lymphocytes (Föger et al., 2006; Mugnier et al., 2008; Shiow et al., 2008). Coro1a is also required for the survival of mycobacteria in phagosomes of infected macrophages (Jayachandran et al., 2007). The role of coronins in the regulation of MC activities is largely unknown.

## RESULTS AND DISCUSSION

To investigate the impact of coronins on MC function, we first determined the expression pattern of coronins. Real-time PCR analysis revealed expression of Coro1a, Coro1b, Coro1c, Coro2a, and Coro7 messenger RNA (mRNA) in MCs, whereas the other coronin family members, Coro2b and Coro6, could not be detected (Fig. S1 a). Within the classical actin regulatory type I coronins, expression was highest for Coro1a and Coro1b, and our further experiments focused on these two coronin proteins. Expression of Coro1a and Coro1b was confirmed on the protein level by Western blotting (Fig. 1 a). Confocal microscopy revealed that Coro1a is primarily localized at the filamentous actin (F-actin)–rich cell cortex in MCs but also exhibits some punctuate cytoplasmic staining, which only minimally colocalized with CD107a $(Lamp1)^+$ secretory lysosomes (Fig. 1 b, 1–9; Fig. S1 f; and Table S2). Cortical localization was instead less pronounced for Coro1b (Fig. 1 b, 10–18).

Importantly, MC stimulation via antigen-specific cross-linking of FcεRI induced the transient phosphorylation of Coro1a and Coro1b on Ser residues, including the regulatory Ser at position 2 (Ser2) of Coro1b (Fig. 1, c and d; and Fig. S1 g), suggesting a regulatory role of Coro1a and Coro1b and, in turn, the actin cytoskeleton in MC function.

We next established IL-3–dependent BM-derived MC (BMMC) cultures from *Coro1a*$^{-/-}$, *Coro1b*$^{-/-}$, and *Coro1a*$^{-/-}$ *Coro1b*$^{-/-}$ mice and compared them with the ones obtained from WT control mice. BMMCs expressed similar levels of selected MC surface markers, c-Kit, FcεRI, and T1/ST2 (Fig. 1 e), and MC-specific genes, such as those encoding for the chymases mMCP-1, mMCP-2, mMCP-5, and mMCP-9, were expressed in similar amounts (Fig. 1 g). Also, the total amount of β-hexosaminidase activity per cell was comparable between all genotypes (Fig. S3 a). Furthermore, Coro1a and/or Coro1b protein was lacking in BMMCs of the respective KO genotype (Fig. 1 f), indicating no compensatory expression between the two coronins family members. A histological analysis also indicated comparable frequency and localization of MCs in different tissues of WT and *Coro1a*$^{-/-}$*Coro1b*$^{-/-}$ mice, as well as normal numbers and morphology of peritoneal MCs (Fig. S2, f–k). These results collectively indicate that MC development is not impaired in the absence of Coro1a and Coro1b.

To evaluate whether Coro1a and Coro1b regulate MC function in vivo, we examined passive cutaneous anaphylaxis (PCA), an MC-dependent, IgE-mediated experimental model which reflects in situ MC mediator release (Inagaki et al., 1986; Wershil et al., 1987). PCA was induced by antigen (DNP human serum albumin [DNP-HSA]) challenge of mice that had been sensitized by intradermal ear injections with anti-DNP IgE. The subsequent assessment of IgE-dependent ear swelling revealed that *Coro1a*$^{-/-}$*Coro1b*$^{-/-}$ mice developed a significantly enhanced PCA reaction compared with WT mice (Fig. 2 a), thus indicating a physiological function of coronin proteins in MC biology and allergic responses.

To provide a cellular basis for the increased cutaneous anaphylaxis in *Coro1a*$^{-/-}$*Coro1b*$^{-/-}$ mice, we examined FcεRI-mediated MC degranulation in coronin-deficient BMMCs by measuring the release of β-hexosaminidase from prestored MC granules. Interestingly, antigen-mediated cross-linking of FcεRI resulted in significantly enhanced release of β-hexosaminidase activity from *Coro1a*$^{-/-}$ BMMCs as compared with WT cells (Fig. 2 b). Although *Coro1b*$^{-/-}$ BMMCs showed normal degranulation, the additional loss of Coro1b further increased hyperdegranulation in *Coro1a*$^{-/-}$ BMMCs. For maximal activation, cells were also stimulated with PMA/ionomycin, which overrides the observed hyperdegranulation phenotype of *Coro1a*$^{-/-}$*Coro1b*$^{-/-}$ BMMCs.

Increased FcεRI-mediated degranulation of *Coro1a*$^{-/-}$ and *Coro1a*$^{-/-}$*Coro1b*$^{-/-}$ BMMCs was further confirmed by assessing the up-regulation of CD107a cell surface expression, which is a marker for granule exocytosis (Fig. 2 c). Again, hyperdegranulation was more pronounced in *Coro1a*$^{-/-}$ *Coro1b*$^{-/-}$ BMMCs compared with *Coro1a*$^{-/-}$ BMMCs, whereas *Coro1b*$^{-/-}$ cells showed no significant difference from WT cells. Together, these data identify Coro1a as a negative regulator of FcεRI-mediated MC degranulation. Furthermore, because the double deficiency of Coro1a and Coro1b exacerbates the *Coro1a*$^{-/-}$ hyperdegranulation phenotype, Coro1b also contributes an overlapping role in regulating MC activities.

To further determine a role of coronins in FcεRI-mediated cytokine secretion, supernatants of BMMCs sensitized with anti-DNP IgE and stimulated with DNP-HSA were collected and tested for cytokine production. IL-6 and TNF secretion was not significantly affected by the single loss of Coro1b (Fig. 2 d). However, in striking contrast to the observed hyperdegranulation of *Coro1a*$^{-/-}$ BMMCs, the release of both IL-6 and TNF was substantially reduced in *Coro1a*$^{-/-}$ BMMCs compared with WT cells (Fig. 2 d), indicating a critical role for Coro1a in FcεRI-mediated cytokine secretion. The additional loss of Coro1b in *Coro1a*$^{-/-}$*Coro1b*$^{-/-}$ BMMCs had no effect on cytokine production. Notably, the reduced detection of IL-6 and TNF in cell supernatants of *Coro1a*$^{-/-}$ and *Coro1a*$^{-/-}$*Coro1b*$^{-/-}$ BMMCs was not secondary to reduced synthesis of these cytokines, as intracellular flow cytometric staining revealed normal to slightly enhanced

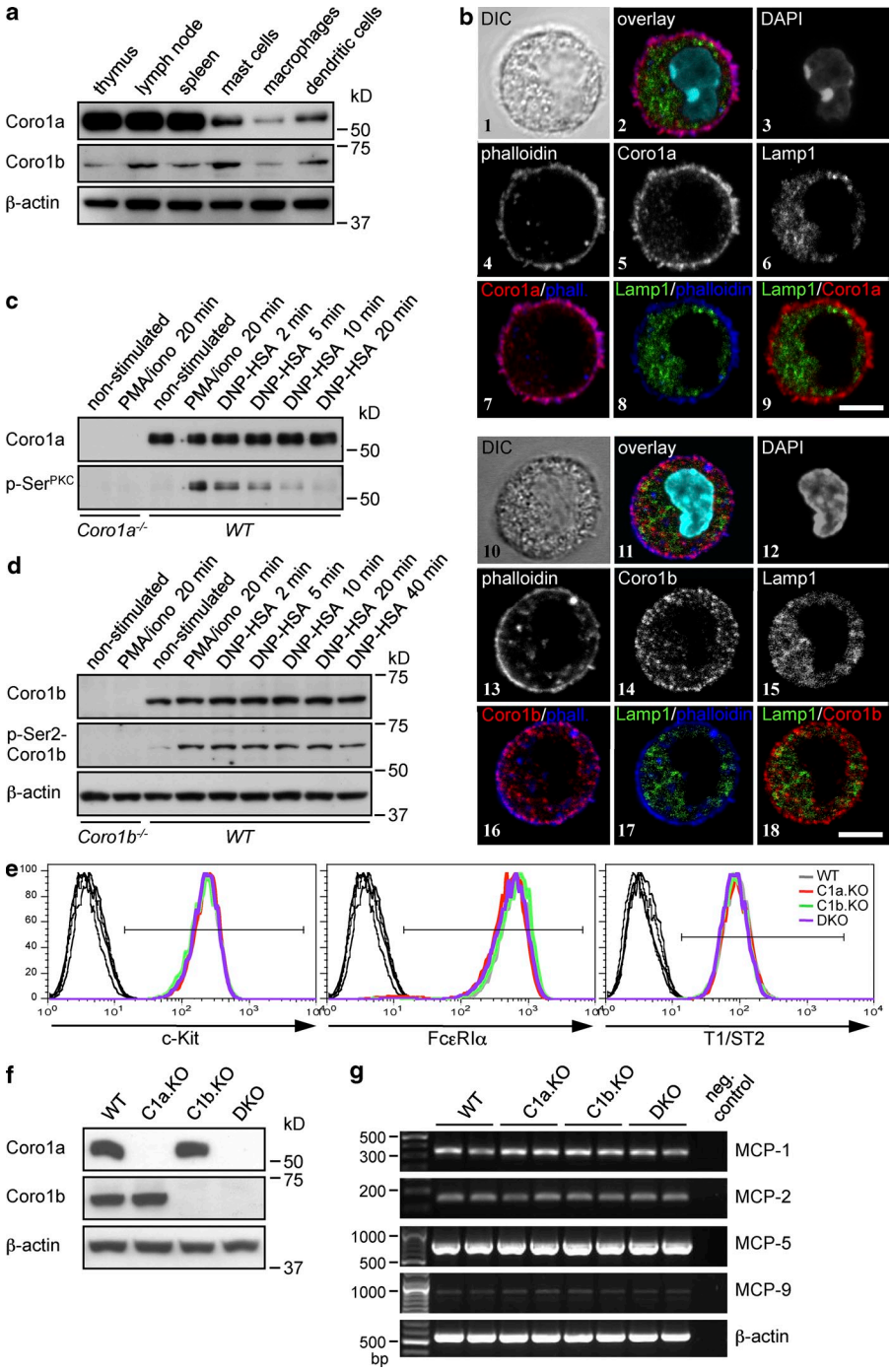


**Figure 1. Expression, localization, and FcεRI-induced Ser phosphorylation of Coro1a and Coro1b in BMMCs.** (a) Immunoblot analysis of Coro1a and Coro1b expression in the indicated tissues or BM-derived cell types. Protein loading was assessed by analysis of β-actin expression throughout the figure. Data are representative of two independent experiments. (b) Subcellular localization of Coro1a and Coro1b in BMMCs. BMMCs were fixed, permeabilized, and stained for either Coro1a (top [1–9]) or Coro1b (bottom [10–18]) together with phalloidin (F-actin), CD107a (Lamp1), and DAPI. Individual and overlay fluorescence images were generated by confocal microscopy and are representative of at least three independent experiments. Bars, 5 µm. (c) Ser phosphorylation of Coro1a in response to FcεRI triggering. WT BMMCs were sensitized with anti-DNP IgE and stimulated with DNP-HSA. Coro1a was immunoprecipitated from lysates at the indicated times and immunoblotted with anti–p-Ser$^{PKC}$ and anti-Coro1a to monitor Coro1a Ser phosphorylation. *Coro1a*$^{-/-}$ BMMCs were used as negative controls. Data are representative of three independent experiments. (d) Phosphorylation of Coro1b on Ser2 in response to FcεRI-mediated BMMC activation. WT BMMCs were sensitized with anti-DNP IgE and stimulated with DNP-HSA for the indicated times. Whole cellular lysates were immunoblotted with anti–p-Coro1b (Ser2) and anti-Coro1b. *Coro1b*$^{-/-}$ BMMCs were used to control for antibody specificity. Data are representative of three independent experiments. (e) Flow cytometric analysis of c-Kit, FcεRI-α, and T1/ST2 surface expression in WT, *Coro1a*$^{-/-}$ (C1a.KO), *Coro1b*$^{-/-}$ (C1b.KO), and *Coro1a*$^{-/-}$*Coro1b*$^{-/-}$ (DKO) BMMCs. Data are representative of at least five independent experiments. (f) Immunoblot analysis of Coro1a and Coro1b expression in BMMCs of the indicated genotype. Data are representative of at least three independent experiments. (g) RT-PCR analysis showing normal expression of mRNA encoding for the MC chymases MCP-1, MCP-2, MCP-5, and MCP-9. Data shown are from two independently generated BMMC lines for each genotype.

expression of IL-6 and TNF in *Coro1a*$^{-/-}$, *Coro1b*$^{-/-}$, and *Coro1a*$^{-/-}$*Coro1b*$^{-/-}$ BMMCs (Fig. 2 e and Fig. S3, e and f). Consistent with these findings, FcεRI-mediated induction of IL-6, IL-13, and TNF mRNA was similar between WT and coronin-deficient BMMCs (Fig. 2 f).

To examine whether coronins are required for IgE-dependent signaling events, FcεRI-induced phosphorylation of the mitogen-activated protein kinases Erk1/Erk2 (Thr202/Tyr204), p38 (Thr180/Tyr182), and JNK1/JNK2 (Thr183/Tyr185) in coronin-deficient and WT BMMCs was investigated. As shown in Fig. 2 g, similar phosphorylation levels and comparable kinetics were observed among BMMCs of all four genotypes. Similarly, normal phosphorylation of the protein kinases Akt (Ser473) and p90Rsk (Ser380; Fig. 2 g) was detected. Because Coro1a has been implicated in the regulation of $Ca^{2+}$ signaling in T lymphocytes (Mueller et al., 2008), we examined the FcεRI-mediated $Ca^{2+}$ influx in *Coro1a*$^{-/-}$*Coro1b*$^{-/-}$ BMMCs and compared it with the one induced in WT BMMCs. However, FcεRI-mediated $Ca^{2+}$ influx was comparable between *Coro1a*$^{-/-}$*Coro1b*$^{-/-}$ and WT BMMCs (Fig. S3 d).

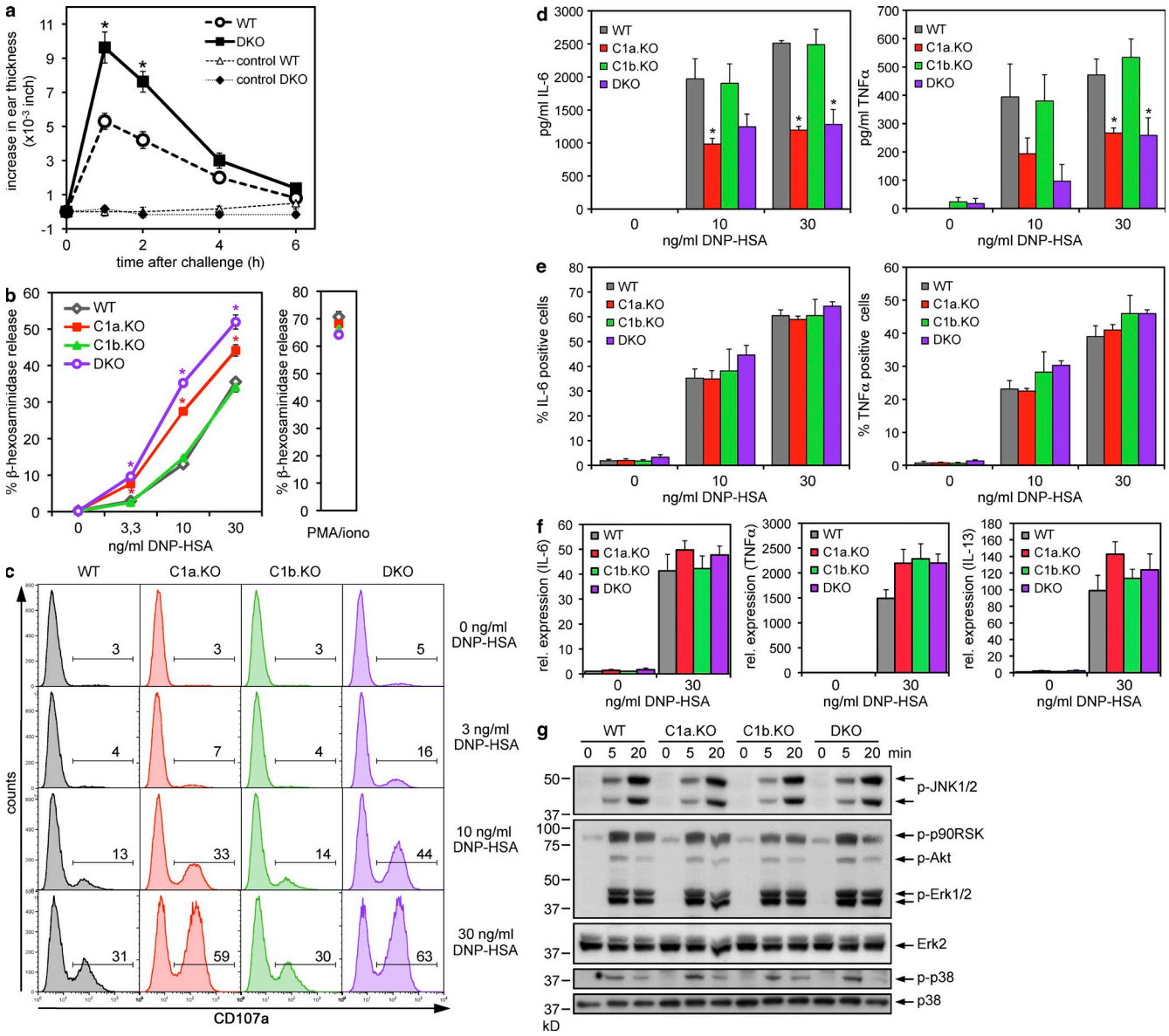


**Figure 2. Coro1a/Coro1b deficiency leads to enhanced IgE-dependent MC degranulation and impaired cytokine production.** (a) Enhanced PCA reaction. Indicated mice received intradermal injections of anti-DNP IgE (or PBS as control) into the ears. After sensitization, mice were i.v. challenged with DNP-HSA as described in Materials and methods. PCA was quantified by monitoring ear thickness. Data are means ± SEM (WT, $n = 5$; DKO, $n = 4$; control treatment, 3 mice each). Results are representative for four independent PCA experiments. *, $P < 0.001$ compared with WT. (b) Increased FcεRI-induced β-hexosaminidase release. WT, *Coro1a*$^{-/-}$ (C1a.KO), *Coro1b*$^{-/-}$ (C1b.KO), and *Coro1a*$^{-/-}$*Coro1b*$^{-/-}$ (DKO) BMMCs were sensitized with anti-DNP IgE and stimulated for 10 min with the indicated concentrations of DNP-HSA. Alternatively, cells were stimulated with PMA/ionomycin. Degranulation was assessed by measuring the release of β-hexosaminidase activity as described in Materials and methods. Data are means ± SD of duplicate cultures and representative of at least three independent experiments. *, $P < 0.001$ compared with WT. (c) Increased FcεRI-induced up-regulation of CD107a surface expression. IgE-sensitized BMMCs were stimulated for 10 min with the indicated concentrations of DNP-HSA. Degranulation was assessed by flow cytometric analysis of CD107a cell surface expression. Numbers shown are the percentage of CD107a-positive cells. Data are representative of at least three independent experiments. (d) Decreased FcεRI-mediated cytokine secretion. Sensitized BMMCs were stimulated for 4 h with the indicated concentrations of DNP-HSA. Release of IL-6 and TNF into the supernatant was measured by ELISA. Data are mean ± SEM from four cultures each. *, $P < 0.05$ compared with WT cells at the indicated antigen concentrations. Data are representative of five independent experiments. (e) Intracellular cytokine production. Sensitized BMMCs were stimulated for 4 h with the indicated concentrations of DNP-HSA in the presence of Brefeldin A. Cells were analyzed for intracellular IL-6 or TNF by flow cytometry, and graphs show the percentage of positive cells ± SEM from two independent experiments. (f) Cytokine gene transcription. Sensitized BMMCs were stimulated for 1 h with DNP-HSA. mRNA levels for IL-6, TNF, and IL-13 were measured by real-time quantitative PCR. The expression level of nonstimulated WT BMMCs was set as 1. Data are mean ± SEM from two independent experiments. (g) FcεRI-induced signaling. Sensitized BMMCs were stimulated with 10 ng/ml DNP-HSA for the indicated times. Whole cellular lysates were subjected to immunoblot analysis using the indicated antibodies. Data are representative of at least three independent experiments.

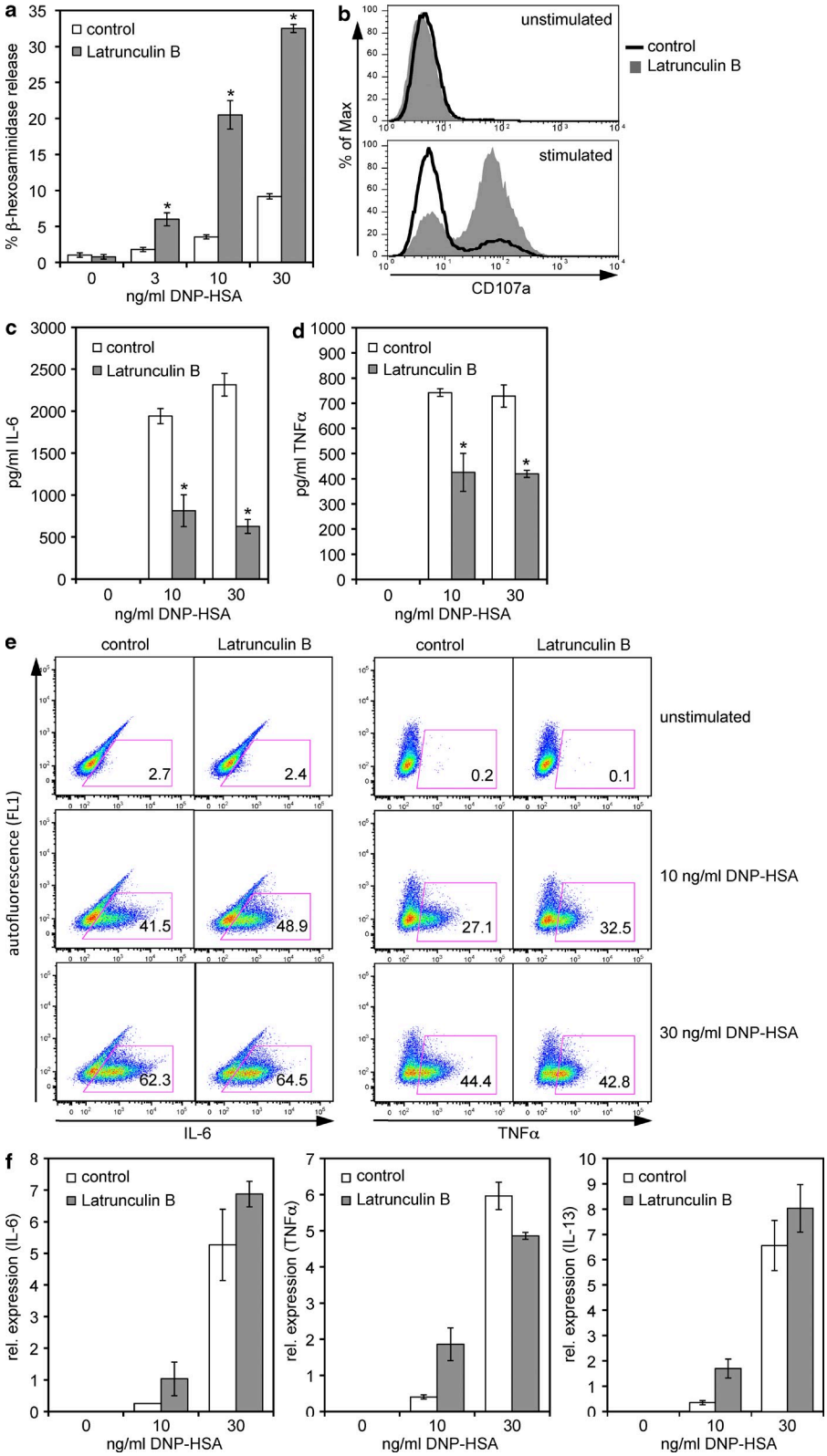


**Figure 3. Dual function of the actin cytoskeleton in the regulation of MC degranulation and cytokine secretion.** (a and b) Increased degranulation in latrunculin B–treated MCs. IgE-sensitized BMMCs pretreated with either 1 µg/ml latrunculin B or carrier (EtOH) were stimulated for 10 min with the indicated concentrations of DNP-HSA (a) or 3 ng/ml DNP-HSA (b). Degranulation was then determined by measuring the release of β-hexosaminidase activity (means ± SD of triplicate samples; a) or flow cytometric analysis of CD107a cell surface expression (b). *, $P < 0.005$ compared with control-treated cells at the indicated antigen concentrations. Data are representative of at least two independent experiments. (c and d) Decreased cytokine secretion in latrunculin B–treated MCs. IgE-sensitized BMMCs pretreated with either 1 µg/ml latrunculin B or carrier (EtOH) were stimulated for 4 h with the indicated concentrations of DNP-HSA. Release of IL-6 (c) and TNF (d) into the supernatant was measured by ELISA (means ± SD of triplicate samples) *, $P < 0.05$ compared with control-treated cells at the indicated antigen concentrations. Data are representative of three independent experiments. (e) Intracellular cytokine production in latrunculin B–treated MCs. Sensitized BMMCs pretreated with either 1 µg/ml latrunculin B or carrier (EtOH) were stimulated for 4 h with the indicated concentrations of DNP-HSA in the presence of Brefeldin A. Cells were analyzed for intracellular IL-6 or TNF by flow cytometry. Data are representative of two independent experiments. (f) Cytokine gene transcription in latrunculin B–treated MCs. Sensitized BMMCs pretreated with either 1 µg/ml latrunculin B or carrier (EtOH) were stimulated for 1 h with DNP-HSA. mRNA levels for IL-6, TNF, and IL-13 were measured by real-time quantitative PCR. Data are mean ± SEM from duplicate samples. Data are representative of two independent experiments.

Together, our data suggest a differential role of coronins in FcεRI-mediated degranulation and cytokine secretion. Furthermore, Coro1b is able to substitute for some functions of Coro1a because hyperdegranulation is aggravated in *Coro1a*$^{-/-}$*Coro1b*$^{-/-}$ BMMCs compared with *Coro1a*$^{-/-}$ cells. In addition, our findings indicate that Coro1a and Coro1b do not affect FcεRI-dependent signaling and cytokine expression in MCs.

To understand whether changes in the actin cytoskeleton are responsible for the differential effect on FcεRI-mediated degranulation and cytokine secretion, we tested the effect of the actin modulatory drug latrunculin B on FcεRI-mediated degranulation. Consistent with previous

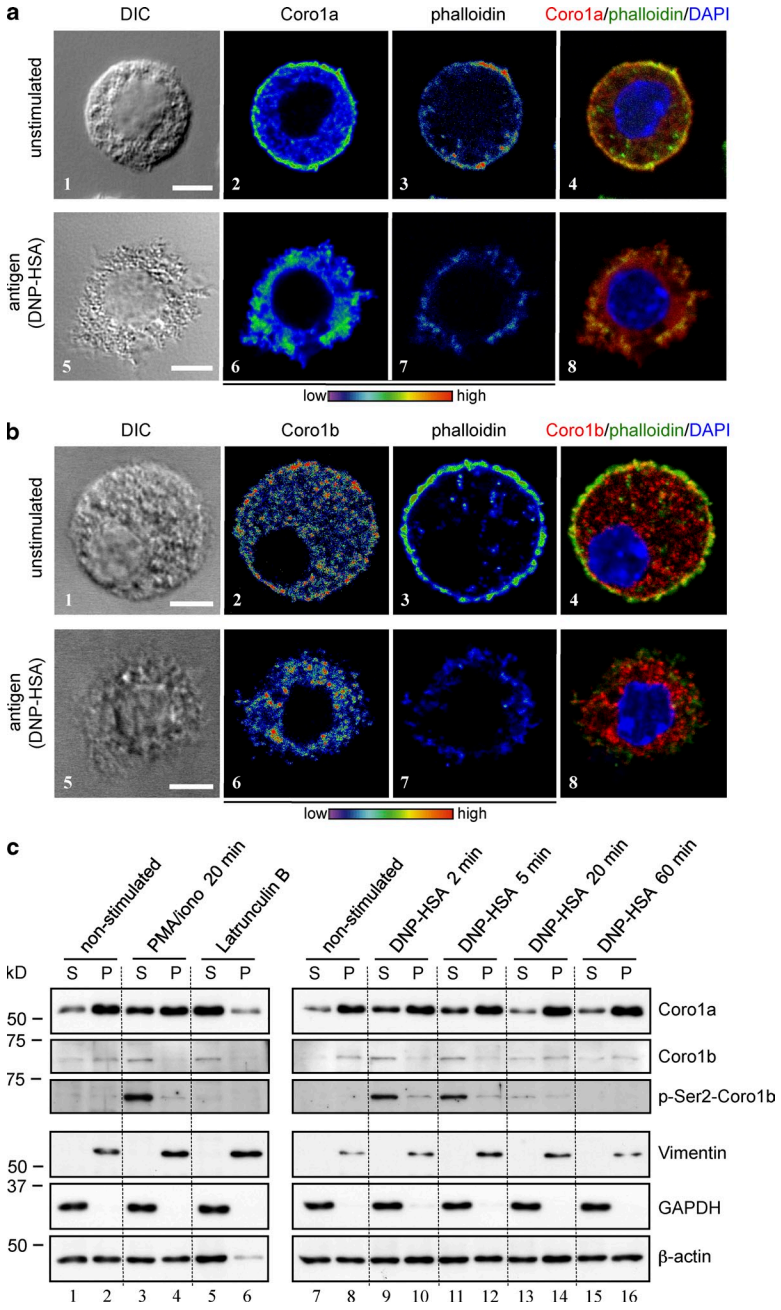


**Figure 4. FcεRI–mediated MC activation induces the subcellular redistribution of Coro1a and Coro1b.** (a and b) Confocal microscopy images showing the subcellular localization of Coro1a (a, 2 and 6) and Coro1b (b, 2 and 6) in unstimulated (1–4) and antigen-stimulated (5–8) BMMCs. Cells were sensitized with anti-DNP IgE (SPE-7) and either stimulated with 75 ng/ml DNP-HSA or control-treated (unstimulated) for 10 min at 37°C. Cells were fixed, permeabilized, and stained for either Coro1a or Coro1b together with phalloidin (F-actin) and DAPI. Representative individual and overlay fluorescence images from two independent experiments are shown. Bars, 5 µm. (c) Biochemical analysis of the subcellular localization of Coro1a and Coro1b. BMMCs either unstimulated or stimulated with PMA/ionomycin (20 min; left) or antigen (75 ng/ml DNP-HSA; 2–60 min; right) were extracted in cytoskeleton isolation buffer as described in Materials and methods. The detergent-insoluble pellet (P; cytoskeletal fraction) and the detergent-soluble supernatant (S; cytosolic fraction) were subjected to immunoblotting using the indicated antibodies. As a control, BMMCs were pretreated with 1 µg/ml latrunculin B (15 min). Data are representative for at least three independent experiments.

studies (Nishida et al., 2005; Sasaki et al., 2005), BMMCs pretreated with latrunculin B exhibited an enhanced degranulation in response to FcεRI cross-linkage, as assessed by measuring β-hexosaminidase release (Fig. 3 a) and by determining the increase in CD107a cell surface staining (Fig. 3 b). Furthermore, contrary to its enhancing effect on MC degranulation, treatment of BMMCs with latrunculin B resulted in decreased secretion of IL-6 and TNF in response to FcεRI stimulation (Fig. 3, c and d). However, intracellular production of these cytokines was not affected by the treatment with latrunculin B, as intracellular FACS staining revealed comparable percentages of IL-6– and TNF-producing cells in latrunculin B– and control-treated BMMCs (Fig. 3 e). Also, the induction of mRNA encoding for IL-6, IL-13, and TNF was similar to slightly enhanced upon treatment of BMMCs with latrunculin B (Fig. 3 f). Collectively, these results suggest that the actin cytoskeleton regulates diverse aspects of MC function. Notably, treatment of BMMCs with latrunculin B mimicked the opposing effects of coronin deficiency on MC degranulation and cytokine secretion.

Coro1a has been linked to the control of the cellular steady-state F-actin content in T cells (Föger et al., 2006). However, in contrast to the massive accumulation of F-actin in *Coro1a*$^{-/-}$ T cells (Föger et al., 2006; Mugnier et al., 2008; Shiow et al., 2008), only minor differences in cellular F-actin levels were observed between WT, *Coro1a*$^{-/-}$, *Coro1b*$^{-/-}$, and *Coro1a*$^{-/-}$*Coro1b*$^{-/-}$ BMMCs (Fig. S4, a and b), reinforcing the idea of cell type– and/or context-specific differences in the actin regulatory activities of coronin proteins (Gandhi et al., 2009). To gain further insights into the role of the actin cytoskeleton and coronin proteins for MC function, we next investigated the intracellular F-actin structure, as well as the subcellular localization of Coro1a and Coro1b upon MC activation by confocal microscopy. MC stimulation induced characteristic changes in cell morphology that are associated with granule release, including cell spreading and the formation of filopodia, membrane ridges, and craters (Fig. 4 a, bottom). Furthermore, MC activation resulted in the disassembly of the cortical F-actin ring (Fig. 4, a and b, 3 and 7). As seen before in unstimulated BMMCs (Fig. 1 b), Coro1a predominantly exhibited a characteristic ring-like staining pattern at the cell periphery, where it colocalized with cortical F-actin (Fig. 4 a). However, after activation of BMMCs, by either stimulation with PMA/ionomycin or antigen-specific

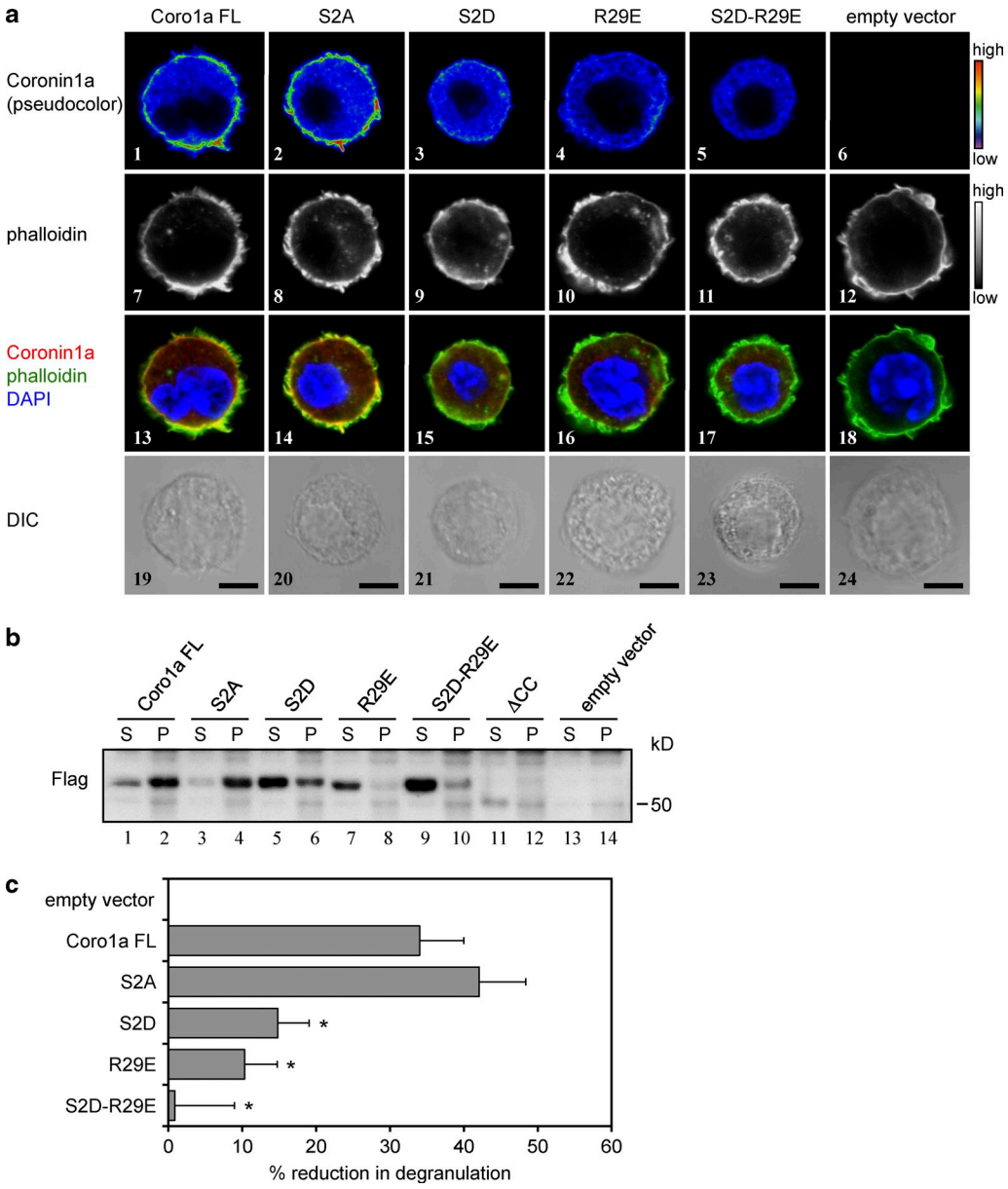


**Figure 5. The inhibitory role of Coro1a on MC degranulation requires the interaction of Coro1a with actin cytoskeletal elements.** (a and b) Subcellular localization of Coro1a mutants. *Coro1a*$^{-/-}$ BMMCs were transfected with Flag-tagged WT (Coro1a FL) or mutant Coro1a internal ribosomal entry site–GFP expression constructs. (a) Cells were fixed, permeabilized, and stained for Coro1a, phalloidin (F-actin), and DAPI. Individual and overlay fluorescence images were obtained by confocal microscopy. Bars, 5 µm. (b) Cells were extracted in cytoskeleton isolation buffer as described in Materials and methods. The detergent-insoluble pellet (P; cytoskeletal fraction) and the detergent-soluble supernatant (S; cytosolic fraction) were subjected to immunoblotting using a Flag-specific antibody. Data are representative for two independent experiments. (c) Functional reconstitution of MC degranulation. *Coro1a*$^{-/-}$*Coro1b*$^{-/-}$ BMMCs were transfected with Flag-tagged WT (C1a) or mutant Coro1a internal ribosomal entry site–GFP expression constructs. Cells were sensitized with anti-DNP IgE and stimulated for 10 min with 10 ng/ml DNP-HSA. MC degranulation was assessed by flow cytometric analysis of CD107a cell surface expression on GFP$^{+}$ (transfected) cells. Results represent the percentage of reduction in CD107a cell surface expression. Expression of coronin constructs was assessed in Fig. S5 a. Data are mean ± SEM of at least three independent experiments. *, $P < 0.05$ compared with Coro1a FL.

cross-linkage of FcεRI, Coro1a relocalized from the cell cortex into the cytoplasm (Fig. 4 a, 6; and Fig. S4 d). Similarly, cortical Coro1b staining also got lost upon MC activation (Fig. 4 b, 6).

An association of Coro1a and Coro1b with the actin cytoskeleton in unstimulated MCs and subcellular relocation of these coronin proteins in response to MC activation was further supported by biochemical fractionation experiments. In nonstimulated BMMCs, Coro1a and Coro1b were predominantly recovered in the detergent-insoluble F-actin–rich pellet (cytoskeletal fraction; Fig. 4 c). Activation of BMMCs by

stimulation with PMA/ionomycin or antigen-specific triggering of FcεRI induced the transient relocation of a substantial amount of Coro1a and Coro1b from the particulate fraction into the cytosolic fraction (Fig. 4 c). The kinetics of the subcellular redistribution of Coro1a and Coro1b upon MC activation resembled the phosphorylation kinetics of Coro1a and Coro1b. Moreover, the subcellular relocation of Coro1b correlated with the detection of Coro1b phosphorylation on Ser2 in the cytosolic fraction (Fig. 4 c). Together, these data suggest that the intracellular distribution of Coro1a and Coro1b in MCs might be determined by their phosphorylation status.

To test this hypothesis, we reconstituted *Coro1a*$^{-/-}$ BMMCs with Flag-tagged Coro1a mutants that affect Coro1a Ser2 phosphorylation and/or its ability to bind F-actin and examined their subcellular localization. As expected, WT Coro1a mainly localized to the F-actin–rich cell cortex (Fig. 5 a, 13) and was predominantly detected in the detergent-insoluble cytoskeletal fraction (Fig. 5 b, lane 2). Similarly, the Coro1a-S2A mutant, which cannot be phosphorylated at Ser2, also exhibited strong colocalization with the actin cytoskeleton (Fig. 5 a, 14). In striking contrast, the phosphomimetic Coro1a-S2D mutant, which lacks Arp2/3-binding activity (Föger et al., 2006), was mainly found in the detergent-soluble cytosolic fraction and showed severely compromised cortical staining (Fig. 5 a, 15). The F-actin–binding mutant Coro1a-R29E (Tsujita et al., 2010) and the Coro1a-S2D-R29E double mutant were almost exclusively detected in the cytoplasmic fraction and exhibited mainly cytoplasmic staining (Fig. 5 a, 16 and 17). Although poorly expressed, Coro1a-ΔCC, which lacks the C-terminal coiled-coil domain, was also primarily found in the cytosolic fraction. Collectively, our data suggest that the cortical localization of Coro1a in BMMCs is largely determined by Ser2 phosphorylation and the F-actin–binding activity of Coro1a.

Next, we investigated the ability of Coro1a mutants to negatively regulate FcεRI-induced degranulation in BMMCs. Reconstitution of *Coro1a*$^{-/-}$*Coro1b*$^{-/-}$ BMMCs with WT Coro1a or Coro1a-S2A resulted in a profound reduction in degranulation, as assessed by CD107a surface staining on transfected (GFP$^{+}$) cells (Fig. 5 c). In marked contrast, hyperdegranulation of *Coro1a*$^{-/-}$*Coro1b*$^{-/-}$ BMMCs was minimally restored by expression of mutant Coro1a-S2D and, even less so, by Coro1a-R29E and Coro1a-S2D-R29E (Fig. 5 c). Together, these results demonstrate that Coro1a negatively regulates MC degranulation via an actin-dependent mechanism.

Our study reveals a dual function of coronin proteins and the actin cytoskeleton on secretory processes in MCs: regulation of MC degranulation and facilitation of cytokine release. Hyperdegranulation of *Coro1a*$^{-/-}$*Coro1b*$^{-/-}$ deficient BMMCs correlates with enhanced cutaneous anaphylaxis in vivo, suggesting a role of coronin proteins in the pathophysiology of allergic disorders. The negative regulatory function of Coro1a on MC degranulation strictly correlates with cortical localization of Coro1a and requires the F-actin–binding site of Coro1a. Interestingly, no alterations in MC function were detected in MCs expressing a truncated mutant of Coro1a (Q262X Coro1a; Arandjelovic et al., 2010), possibly because of some residual regulatory activity of the mutant Coro1a protein. We propose that Coro1a exhibits no major effects on steady-state actin polymerization in unstimulated MCs but rather stabilizes the cortical network of actin filaments via its actin-binding and/or -bundling activity, thereby entrapping secretory granules and preventing unwanted granule release. This idea is consistent with the recently described F-actin decoration and stabilization function of Coro1A (Galkin et al., 2008). Actin-dependent processes have further been implicated in the regulation of membrane trafficking from the ER to the Golgi and the plasma membrane (Müsch et al., 1997), a cellular transport route which is also used for release of newly synthesized cytokines. Normal synthesis but reduced secretion of cytokines in *Coro1a*$^{-/-}$ MCs thus suggests that owing to its actin-regulatory function, Coro1a is involved in the control of vesicular trafficking in MCs. Together, our data provide genetic evidence to support the longstanding hypothesis that the cortical actin network acts as a physical barrier to prevent docking and fusion of secretory granules to the plasma membrane (Aunis and Bader, 1988).

Exocytosis is accompanied by a regulated reorganization of cortical actin filaments, which is then thought to allow for recruitment of granules to exocytic sites (Eitzen, 2003). Our data suggest that Coro1a and Coro1b are functionally involved in the stimulus-dependent control of the stability and the dynamics of the cortical actin network. FcεRI triggering induces the subcellular relocation of Coro1a and Coro1b from the actin-rich cell cortex to the cytoplasm, thereby likely contributing to reduced cortical stability and better access of secretory granules to the plasma membrane upon cellular activation. This intracellular redistribution of Coro1a and Coro1b in MCs is regulated by FcεRI-mediated phosphorylation of Coro1a and Coro1b on the critical Ser2. This phosphorylation event has previously been demonstrated to reduce the interaction with the Arp2/3 complex (Cai et al., 2005; Föger et al., 2006), which is a central component of the actin cytoskeleton. Thus, Ser2-phosphorylated coronin exhibits reduced binding to the cortical actin network, which likely annihilates the actin-dependent negative regulatory function of coronin on MC degranulation. Despite the high degree of sequence conservation between coronin family members, Coro1b only partially compensates for Coro1a deficiency in MC degranulation and, in contrast to Coro1a, has no discernable effect on cytokine release. Thus, our findings indicate that coronin family members have developed both common and specialized functions.

In conclusion, distinct secretory pathways have fundamentally different requirements on coronin proteins and the actin cytoskeleton in MCs. These findings likely represent common regulatory themes that also apply to other secretory cells. Additional mechanistic studies will further reveal the specific modalities of actin regulation for exocytic processes under normal and pathophysiological conditions.

## MATERIALS AND METHODS

**Mice.** Coro1a-deficient mice were reported previously (Föger et al., 2006). Coro1b-deficient mice were generated using homologous recombination in embryonic stem cells as described in Fig. S2 a. Heterozygous mice were backcrossed for >10 generations onto C57BL/6N mice. Coro1a/Coro1b double-deficient mice were obtained by interbreeding Coro1a- and Coro1b-deficient mice. Mice were housed under specific pathogen–free conditions at the Animal Care Facility of the Research Center Borstel. Animal experiments were performed in accordance with institutional guidelines and were approved by the local authorities (Ministry of Agriculture, the Environment, and Rural Areas, Schleswig-Holstein).

**Antibodies and reagents.** Fluorescent labeled antibodies specific for c-Kit, FcεRIα, TNF, IL-6, CD3, CD11b, CD11c, CD107a, and B220 were all obtained from eBioscience, and anti-T1/ST2 was obtained from MD Biosciences. Anti-DNP IgE (SPE-7) was purchased from Sigma-Aldrich. Antibodies to p-Ser$^{PKC}$ (phospho-[Ser] PKC substrate), p-JNK1/2 (Thr183/Tyr185), p-p90Rsk (Ser380), p-Akt (Ser473), p-Erk1/2 (Thr202/Tyr204), p-p38 (Thr180/Tyr182), and p38 were obtained from Cell Signaling Technology. Antibodies to GAPDH (6C5), Erk-2 (C-14), and β-actin were purchased from Santa Cruz Biotechnology, Inc. Vimentin-specific antibody and FcBlock (anti-CD16/CD32) were obtained from BD. Anti–p-Ser2-Coro1b was purchased from ECM Biosciences. Antibodies to Coro1a and Coro1b have been described previously (Föger et al., 2006). Fluorescent-labeled secondary antibodies were obtained from Jackson ImmunoResearch Laboratories, Inc. PMA and ionomycin were both purchased from Sigma-Aldrich. Latrunculin B was obtained from Enzo Life Sciences.

**PCA.** For the induction of PCA, mice were sensitized by intradermal injection in both ears of 10 µl anti-DNP IgE (SPE-7) diluted in PBS (50 ng IgE per ear, twice) or PBS as a control. Mice were challenged by i.v. injection of 200 µg DNP-HSA (Sigma-Aldrich) in 100 µl PBS 48 h later. Ear thickness was measured before antigen injection and 1, 2, 4, and 6 h after antigen injection using a dial thickness gauge (Mitutoyo). The researcher conducting the in vivo experiments was blinded to the experimental design.

**Cell isolation, generation, culture, and activation.** Peritoneal cells were isolated by peritoneal lavage with 10 ml of cold 0.9% NaCl solution. BMMCs were prepared as described previously (Orinska et al., 2007). In brief, BM cells were flushed from femurs, and the MCs were selectively grown in MC medium (IMDM supplemented with 10% FBS, 50 µM β-mercaptoethanol, 2 mM L-glutamine, penicillin, streptomycin, nonessential amino acids, vitamins, and Na-pyruvate) in the presence of 10 ng/ml recombinant IL-3 (R&D Systems) for 5–10 wk. Cell purity was routinely checked by flow cytometric analysis of c-Kit, FcεRI-α, and T1/ST2 cell surface expression. After sensitization of the cells overnight with 200 ng/ml anti-DNP IgE (SPE-7) in MC medium containing 1 ng/ml IL-3, cells were activated with the indicated concentrations of DNP-HSA. Where indicated, cells were preincubated with 1 µg/ml latrunculin B for 15 min at 37°C. BM-derived macrophages and BM-derived DCs were differentiated by culturing BM cells for 8–9 d in the presence of either 20 ng/ml M-CSF (BM-derived macrophages) or 20 ng/ml GM-CSF (BM-derived DCs).

**Flow cytometric analysis.** Single cell suspensions of BMMCs were blocked with FcBlock (anti-CD16/CD32; BD) and subsequently stained with fluorescent-labeled mAbs. To assess the cellular F-actin content, cells were fixed in 4% paraformaldehyde (PFA) in PBS, permeabilized with 0.2% Triton X-100, and stained with fluorescence-conjugated phalloidin (Invitrogen). Intracellular staining of cytokines was performed in permeabilized cells according to standard procedures. Flow cytometric measurements were performed on a FACSCalibur and an LSRII (both BD). Data were analyzed with FlowJo software (version 8.8.6; Tree Star).

**Measurement of degranulation.** MC degranulation was assessed by measuring the release of β-hexosaminidase activity (Orinska et al., 2010). In brief, sensitized cells were activated with DNP-HSA in Tyrode's buffer (10 mM Hepes, pH 7.4, 130 mM NaCl, 5 mM KCl, 1.4 mM $CaCl_2$, 1 mM $MgCl_2$, 5.6 mM glucose, and 0.1% [wt/vol] BSA). Supernatant or cell pellets solubilized with 1% Triton X-100 in Tyrode's buffer were incubated with p-nitrophenyl-N-acetyl-D-glucosamide (Sigma-Aldrich; 1.3 mg/ml in 0.1 M citrate, pH 4.5), and color was developed for 30 min at 37°C. The enzyme reaction was stopped by the addition of 0.2 M Gly-NaOH, pH 10.7, and the absorbance at 405 nm was measured. The percentage of β-hexosaminidase released was calculated by dividing the absorbance in the supernatant by the sum of the absorbance in the supernatant and detergent-solubilized cell pellet. Statistical analysis was performed by two-tailed Student's *t* test. Degranulation was also assessed by flow cytometric measurement of the surface expression of CD107a (Lamp1).

**Measurement of cytokines.** Sensitized BMMCs were stimulated with DNP-HSA for 4 h at 37°C, and cytokines in cell supernatants were analyzed by ELISA. Coating and detection antibodies for TNF and IL-6 and protein standards were purchased from R&D Systems. For the detection of intracellular cytokines, cells were stimulated for 4 h in the presence of Brefeldin A (eBioscience) for blockade of Golgi function. Cells were fixed with 4% PFA in PBS, permeabilized, and subjected to intracellular FACS staining using antibodies against IL-6 and TNF.

**Immunofluorescence microscopy.** Cells were fixed with 4% PFA and permeabilized with 0.2% Triton X-100 in PBS. After blocking, immunofluorescence labeling was performed according to standard procedures using directly labeled antibodies against Coro1a and CD107a (Lamp1). Coro1b was detected by using anti–hamster IgG-DyLight649 secondary antibody. Specificity of the coronin staining was confirmed by using *Coro1a*$^{-/-}$ or *Coro1b*$^{-/-}$ BMMCs as controls. F-actin and DNA were visualized by staining with phalloidin (Invitrogen) and DAPI (Invitrogen), respectively. Confocal images were acquired on a microscope (TCS Sp5; Leica). Subsequent image analysis was performed using iVision software (BioVision Technologies). For each staining, at least 50–100 cells were analyzed. Selected pictures show patterns that were representative for at least 75% of cells (for stimulated conditions, only cells that showed signs of cellular activation were considered). The Pearson's correlation coefficient as a measure for the extent of colocalization was calculated using iVisionEvaluation software (BioVision Technologies).

**RT-PCR and real-time quantitative RT-PCR analysis.** Total RNA was purified from BMMCs using the RNeasy system (QIAGEN) according to the manufacturer's instructions and reverse transcribed using the Superscript II first-strand synthesis system (Invitrogen). For some experiments, the FastLane cDNA kit (QIAGEN) was used. Primers and conditions for standard PCR to detect MC proteases were described previously (Orinska et al., 2010). Mouse MCP-1 was detected with sense (5′-AAAGCCCCCTGCAGTCTTCACC-3′) and antisense (5′-AGCTGCTGGAGGTTAGGTC-3′) primers. PCR products were separated on an agarose gel, stained with ethidium bromide, and photographed. For real-time quantitative RT-PCR, IL-6, TNF, and IL-13 gene expression was measured relative to HPRT using the Universal ProbeLibrary (Roche) TaqMan-based system. Amplification was performed in a fluorescence temperature cycler (Light Cycler 2.0; Roche). Primers and the Universal ProbeLibrary ID numbers are listed in Table S1.

**Western blotting and immunoprecipitation.** After stimulation of sensitized BMMCs with DNP-HSA or PMA/ionomycin, cells were lysed in cell extraction buffer: 1% NP-40, 50 mM Tris-HCl buffer, pH 8.0, 150 mM NaCl, 10 mM Na fluoride, 1 mM Na orthovanadate, and protease inhibitors (complete protease inhibitor cocktail; Roche). For immunoprecipitation experiments, cell lysates were precleared with protein A beads and subsequently incubated for 1–2 h with protein A beads covalently coupled with anti-Coro1a mAb. Immune complexes were washed four times with cell extraction buffer. Eluted samples or whole cellular lysates were resolved by SDS-PAGE, and proteins were detected by Western blotting using the

indicated antibodies. Densitometric analysis was performed using ImageJ software (National Institutes of Health; Tables S3–S9).

**Isolation of the cytoskeleton-rich fraction.** Subcellular fractionation and isolation of the cytoskeleton-containing detergent-insoluble fraction was performed according to Gatfield et al. (2005). In brief, cell pellets ($10^6$ cells) were suspended in 0.3 ml of ice-cold cytoskeletal isolation buffer (1% Triton X-100 in 80 mM Pipes, pH 6.8, 5 mM EGTA, and 1 mM $MgCl_2$) and immediately centrifuged at 3,000 *g* for 3 min to obtain the detergent-insoluble cytoskeleton-containing fraction and the detergent-soluble cytosolic fraction. Equal cell equivalents were subjected to SDS-PAGE and Western blotting.

**Expression constructs and transient transfection of BMMCs.** Coronin expression constructs were cloned into the bicistronic expression vector pIRES2-EGFP (Takara Bio Inc.). Full-length mouse Coro1a (aa 1–461) carrying a C-terminal Flag tag, as well as Coro1a-S2A and Coro1a-S2D mutants and the coiled-coil deletion (ΔCC) mutant of Coro1a have been described previously (Föger et al., 2006). The actin-binding mutant Coro1a-R29E (Tsujita et al., 2010) and the Coro1a-S2D-R29E double mutant were generated using the QuikChange site-directed mutagenesis kit (Agilent Technologies). Constructs were transfected into BMMCs using the Nucleofector system (solution T and program T-16) according to the method described by Jeffrey et al. (2006). After transfection, cells were allowed to recover for 24 h in MC medium containing 1 ng/ml IL-3. Cells were then sensitized with anti–DNP-HSA and stimulated with DNP-HSA. MC degranulation was assessed by flow cytometric analysis of CD107a cell surface expression. Transfected cells were identified on the basis of their GFP expression. Dead cells were excluded by propidium iodide staining. FcεRI-induced degranulation in control-transfected cells (empty vector control) was >20% in all of the experiments. Equal expression levels of coronin constructs in transfected BMMCs were controlled by intracellular FACS staining for Coro1a (Fig. S5 a).

**Online supplemental material.** Fig. S1 shows mRNA expression levels of coronin family members in different tissues and cell types, demonstrates the specificity of the Coro1a and Coro1b staining in confocal microscopy experiments, and also shows reduced activation-induced Ser phosphorylation of the Coro1a-S2A mutant compared with WT Coro1a. Fig. S2 describes the generation of Coro1b-deficient mice, shows the expression of Coro1a and Cora1b in peritoneal MCs, and demonstrates normal in vivo development of *Coro1a*$^{-/-}$*Coro1b*$^{-/-}$ MCs. Fig. S3 shows the total cellular β-hexosaminidase content, as well as FcεRI-induced degranulation, calcium mobilization, and intracellular cytokine production in WT and coronin-deficient BMMCs. Fig. S4 depicts relative cellular F-actin contents in naive $CD4^+$ T cells and BMMCs, as well as relative changes in F-actin levels upon FcεRI stimulation and the subcellular redistribution of Coro1a upon MC activation. Fig. S5 shows functional reconstitution of MC degranulation upon expression of different coronin constructs in *Coro1a*$^{-/-}$*Coro1b*$^{-/-}$ BMMCs. Table S1 describes primers and Universal ProbeLibrary ID numbers used for quantitative real-time PCR analysis. Table S2 provides an analysis of confocal pictures by determining the Pearson's correlation coefficient as a measure of colocalization. Tables S3–S9 show the densitometric analysis of immunoblots. Online supplemental material is available at http://www.jem.org/cgi/content/full/jem.20101757/DC1.

We thank Manuel Hein for excellent technical support and also greatly appreciate the help of Katrin Streeck and Katrin Westphal.

This work was funded in part by grants from the Deutsche Forschungsgemeinschaft to S. Bulfone-Paus (SFB/TR 22, A14).

A.C. Chan is an employee of Genentech. The authors declare that they have no other competing financial interests.

**Submitted: 23 August 2010**
**Accepted: 7 July 2011**

## REFERENCES

Arandjelovic, S., D. Wickramarachchi, S. Hemmers, S.S. Leming, D.H. Kono, and K.A. Mowen. 2010. Mast cell function is not altered by Coronin-1A deficiency. *J. Leukoc. Biol.* 88:737–745. doi:10.1189/jlb.0310131

Aunis, D., and M.F. Bader. 1988. The cytoskeleton as a barrier to exocytosis in secretory cells. *J. Exp. Biol.* 139:253–266.

Blank, U., and J. Rivera. 2004. The ins and outs of IgE-dependent mast-cell exocytosis. *Trends Immunol.* 25:266–273. doi:10.1016/j.it.2004.03.005

Brown, J.M., T.M. Wilson, and D.D. Metcalfe. 2008. The mast cell and allergic diseases: role in pathogenesis and implications for therapy. *Clin. Exp. Allergy.* 38:4–18.

Cai, L., N. Holoweckyj, M.D. Schaller, and J.E. Bear. 2005. Phosphorylation of coronin 1B by protein kinase C regulates interaction with Arp2/3 and cell motility. *J. Biol. Chem.* 280:31913–31923. doi:10.1074/jbc.M504146200

Cai, L., A.M. Makhov, and J.E. Bear. 2007a. F-actin binding is essential for coronin 1B function in vivo. *J. Cell Sci.* 120:1779–1790. doi:10.1242/jcs.007641

Cai, L., T.W. Marshall, A.C. Uetrecht, D.A. Schafer, and J.E. Bear. 2007b. Coronin 1B coordinates Arp2/3 complex and cofilin activities at the leading edge. *Cell.* 128:915–929. doi:10.1016/j.cell.2007.01.031

Clemen, C.S., V. Rybakin, and L. Eichinger. 2008. The coronin family of proteins. *Subcell. Biochem.* 48:1–5. doi:10.1007/978-0-387-09595-0_1

Eitzen, G. 2003. Actin remodeling to facilitate membrane fusion. *Biochim. Biophys. Acta.* 1641:175–181. doi:10.1016/S0167-4889(03)00087-9

Föger, N., L. Rangell, D.M. Danilenko, and A.C. Chan. 2006. Requirement for coronin 1 in T lymphocyte trafficking and cellular homeostasis. *Science.* 313:839–842. doi:10.1126/science.1130563

Frigeri, L., and J.R. Apgar. 1999. The role of actin microfilaments in the down-regulation of the degranulation response in RBL-2H3 mast cells. *J. Immunol.* 162:2243–2250.

Galkin, V.E., A. Orlova, W. Brieher, H.Y. Kueh, T.J. Mitchison, and E.H. Egelman. 2008. Coronin-1A stabilizes F-actin by bridging adjacent actin protomers and stapling opposite strands of the actin filament. *J. Mol. Biol.* 376:607–613. doi:10.1016/j.jmb.2007.12.007

Gandhi, M., V. Achard, L. Blanchoin, and B.L. Goode. 2009. Coronin switches roles in actin disassembly depending on the nucleotide state of actin. *Mol. Cell.* 34:364–374. doi:10.1016/j.molcel.2009.02.029

Gatfield, J., I. Albrecht, B. Zanolari, M.O. Steinmetz, and J. Pieters. 2005. Association of the leukocyte plasma membrane with the actin cytoskeleton through coiled coil-mediated trimeric coronin 1 molecules. *Mol. Biol. Cell.* 16:2786–2798. doi:10.1091/mbc.E05-01-0042

Humphries, C.L., H.I. Balcer, J.L. D'Agostino, B. Winsor, D.G. Drubin, G. Barnes, B.J. Andrews, and B.L. Goode. 2002. Direct regulation of Arp2/3 complex activity and function by the actin binding protein coronin. *J. Cell Biol.* 159:993–1004. doi:10.1083/jcb.200206113

Inagaki, N., S. Goto, M. Yamasaki, H. Nagai, and A. Koda. 1986. Studies on vascular permeability increasing factors involved in 48-hour homologous PCA in the mouse ear. *Int. Arch. Allergy Appl. Immunol.* 80:285–290. doi:10.1159/000234067

Jayachandran, R., V. Sundaramurthy, B. Combaluzier, P. Mueller, H. Korf, K. Huygen, T. Miyazaki, I. Albrecht, J. Massner, and J. Pieters. 2007. Survival of mycobacteria in macrophages is mediated by coronin 1-dependent activation of calcineurin. *Cell.* 130:37–50. doi:10.1016/j.cell.2007.04.043

Jeffrey, K.L., T. Brummer, M.S. Rolph, S.M. Liu, N.A. Callejas, R.J. Grumont, C. Gillieron, F. Mackay, S. Grey, M. Camps, et al. 2006. Positive regulation of immune cell function and inflammatory responses by phosphatase PAC-1. *Nat. Immunol.* 7:274–283. doi:10.1038/ni1310

Kalesnikoff, J., and S.J. Galli. 2008. New developments in mast cell biology. *Nat. Immunol.* 9:1215–1223. doi:10.1038/ni.f.216

Kinet, J.P. 2007. The essential role of mast cells in orchestrating inflammation. *Immunol. Rev.* 217:5–7. doi:10.1111/j.1600-065X.2007.00528.x

Kueh, H.Y., G.T. Charras, T.J. Mitchison, and W.M. Brieher. 2008. Actin disassembly by cofilin, coronin, and Aip1 occurs in bursts and is inhibited by barbed-end cappers. *J. Cell Biol.* 182:341–353. doi:10.1083/jcb.200801027

Malacombe, M., M.-F. Bader, and S. Gasman. 2006. Exocytosis in neuroendocrine cells: new tasks for actin. *Biochim. Biophys. Acta.* 1763:1175–1183. doi:10.1016/j.bbamcr.2006.09.004

Mueller, P., J. Massner, R. Jayachandran, B. Combaluzier, I. Albrecht, J. Gatfield, C. Blum, R. Ceredig, H.R. Rodewald, A.G. Rolink, and J. Pieters. 2008. Regulation of T cell survival through coronin-1-mediated generation of inositol-1,4,5-trisphosphate and calcium mobilization after T cell receptor triggering. *Nat. Immunol.* 9:424–431. doi:10.1038/ni1570

Mugnier, B., B. Nal, C. Verthuy, C. Boyer, D. Lam, L. Chasson, V. Nieoullon, G. Chazal, X.-J. Guo, H.-T. He, et al. 2008. Coronin-1A links cytoskeleton dynamics to TCR alpha beta-induced cell signaling. *PLoS ONE.* 3:e3467. doi:10.1371/journal.pone.0003467

Müsch, A., D. Cohen, and E. Rodriguez-Boulan. 1997. Myosin II is involved in the production of constitutive transport vesicles from the TGN. *J. Cell Biol.* 138:291–306. doi:10.1083/jcb.138.2.291

Nishida, K., S. Yamasaki, Y. Ito, K. Kabu, K. Hattori, T. Tezuka, H. Nishizumi, D. Kitamura, R. Goitsuka, R.S. Geha, et al. 2005. FcεRI-mediated mast cell degranulation requires calcium-independent microtubule-dependent translocation of granules to the plasma membrane. *J. Cell Biol.* 170:115–126. doi:10.1083/jcb.200501111

Orinska, Z., M. Maurer, F. Mirghomizadeh, E. Bulanova, M. Metz, N. Nashkevich, F. Schiemann, J. Schulmistrat, V. Budagian, J. Giron-Michel, et al. 2007. IL-15 constrains mast cell-dependent antibacterial defenses by suppressing chymase activities. *Nat. Med.* 13:927–934. doi:10.1038/nm1615

Orinska, Z., N. Föger, M. Huber, J. Marschall, F. Mirghomizadeh, X. Du, M. Scheller, P. Rosenstiel, T. Goldmann, A. Bollinger, et al. 2010. I787 provides signals for c-Kit receptor internalization and functionality that control mast cell survival and development. *Blood.* 116:2665–2675. doi:10.1182/blood-2009-06-228460

Sasaki, J., T. Sasaki, M. Yamazaki, K. Matsuoka, C. Taya, H. Shitara, S. Takasuga, M. Nishio, K. Mizuno, T. Wada, et al. 2005. Regulation of anaphylactic responses by phosphatidylinositol phosphate kinase type I α. *J. Exp. Med.* 201:859–870. doi:10.1084/jem.20041891

Shiow, L.R., D.W. Roadcap, K. Paris, S.R. Watson, I.L. Grigorova, T. Lebet, J. An, Y. Xu, C.N. Jenne, N. Föger, et al. 2008. The actin regulator coronin 1A is mutant in a thymic egress-deficient mouse strain and in a patient with severe combined immunodeficiency. *Nat. Immunol.* 9:1307–1315. doi:10.1038/ni.1662

Tsujita, K., T. Itoh, A. Kondo, M. Oyama, H. Kozuka-Hata, Y. Irino, J. Hasegawa, and T. Takenawa. 2010. Proteome of acidic phospholipid-binding proteins: spatial and temporal regulation of Coronin 1A by phosphoinositides. *J. Biol. Chem.* 285:6781–6789. doi:10.1074/jbc.M109.057018

Uetrecht, A.C., and J.E. Bear. 2006. Coronins: the return of the crown. *Trends Cell Biol.* 16:421–426. doi:10.1016/j.tcb.2006.06.002

Wershil, B.K., Y.A. Mekori, T. Murakami, and S.J. Galli. 1987. 125I-fibrin deposition in IgE-dependent immediate hypersensitivity reactions in mouse skin. Demonstration of the role of mast cells using genetically mast cell-deficient mice locally reconstituted with cultured mast cells. *J. Immunol.* 139:2605–2614.